Cadmium trapping by C60 and B-, Si-, and N-doped C60

Kuganathan, N., Selvanantharajah, N., Iyngaran, P., Abiman, P. & Chroneos, A.

Cadmium Trapping by C_{60} and B−, Si− and N−Doped C_{60}

Navaratnarajah Kuganathan[1,a)], Namasivayam Selvanantharajah[2], Poobalasuntharam Iyngaran[2], Poobalasingam Abiman[2] and Alexander Chroneos[1,3,b)]

[1]Department of Materials, Imperial College London, London, SW7 2AZ, United Kingdom

[2]Depratment of Chemistry, University of Jaffna, Sir Pon Ramanathan Road, Thirunelvely, Jaffna, Srilanka

[3]Faculty of Engineering, Environment and Computing, Coventry University, Priory Street, Coventry CV1 5FB, United Kingdom

_____

Abstract

Removal of heavy metals from the environment has attracted considerable attention as they are toxic and non-biodegradable or destroyable. To minimize their hazard, they should be removed through either physical or chemical capture. Cadmium is a heavy metal that can lead to severe risks to human health. Using density functional theory with a dispersion correction (DFT+D), we predict the structures and energies of Cd trapped by C_{60}. Furthermore, we substitutionally doped C_{60} with a single B, Si and N and examined its trapping behaviour. The lowest substitutional energy was calculated for B. Significant enhancement in trapping is observed with B and Si doping outside the surface in particular and our results warrant further experimental investigation.

[1]Corresponding authors, e-mails: a) n.kuganathan@imperial.ac.uk ; b) alexander.chroneos@imperial.ac.uk

1. Introduction

Rapid industrial usage of heavy metals such as cadmium, lead, copper, zinc and mercury pollutes environment directly or indirectly. Industrial activities such as electroplating, smelting, mining and manufacturing batteries and fertilisers etc., increase the level of toxic heavy metals in the aqueous environment with the possible risk of damaging human physiology.[1] As heavy metals cannot be biodegradable or destroyable unlike organic contaminants, its acceptable level concentration exceeds and results further damage to the environment.

Cadmium is one of the toxic heavy metals mainly found in cigarette smoke,[2] tap water,[3] and seafood[4]. Due to its very low excretion from the body at high level it exposes human health to severe risks. It mainly damages kidneys[5] and cardiovascular system[6]. Thus there is a necessity to remove cadmium especially from water and air. Significant effort has been devoted to find ways to remove heavy metals using methods such as ion exchange,[7] solvent extraction,[8] coagulation,[9] adsorption,[10] chemical precipitation and reverse osmosis.[11] Several sorbents including activated carbon,[12] carbon nanotubes,[13] chemically modified carbon,[10] zeolites[14] and biomass[15] have been studied experimentally to remove heavy metals from water.

The buckyball (C_{60}) or its modified form (e.g. doped C_{60}) is a candidate material to trap cadmium as it provides both inner and outer surface structures. In addition, its high resistance to external chemical attack, light weight and high mechanical stability at high pressure and temperatures attract C_{60} as a potential sorbent[16]. There are experimental and theoretical studies on alkali metals,[17-19] alkali earth metals,[17,20] radioactive isotopes,[21,22] actinide metals,[23] non-metals,[24,25] noble gases,[18] transition metals, [26,27]rare earth metals[28] and metal clusters[19,27].

Using density functional theory (DFT) together with dispersion corrections (DFT+D), the thermodynamic stability of cadmium with inner and outer surface of C_{60} is investigated. Furthermore B, Si and N is substitutionally doped and the stability of Cd is discussed. DFT calculations, in addition to giving structural information, provide electronic structure and properties.

2. Computational Methods

Calculations were carried out using the spin-polarized mode of DFT as implemented in the VASP [29,30] package. The exchange-correlation term was modelled using the generalized gradient approximation (GGA) parameterized by Perdew, Burke, and Ernzerhof (PBE)[31]. In

all cases, we have used a plane-wave basis set with a cut-off value of 500 eV. Further increase in the plane wave-basis set cut off would increase the computational time. In our previous study[18], we have tested 500 eV is sufficient for the convergence. Structural optimisations were performed using a conjugate gradient algorithm[32] and the forces on the atoms were obtained via the Hellman-Feynmann theorem including Pulay corrections. In all optimized structures, forces on the atoms were smaller than 0.001 eV/Å and all the values in the atomic stress tensor were less than 0.002 GPa. All geometry optimisations were performed using a single k-point as C_{60} is treated as a molecule and additional k-points did not make any significant difference in total energy . A cubic supercell with a length of 20 Å was used for all configurations to ensure that adjacent structures do not interact (the largest linear dimension of a C_{60} molecule was 7.10 Å). One of the limitations in this methodology is the size of the supercell. The larger supercell means a large number of plane wave basis sets with high computational time. We define encapsulation energy for single Cd atom trapping inside the cage and association energy for single Cd atom trapping outside the cage by the following equation:

$$E_{Enc/Assoc} = E\ (Cd\text{-}C_{60}) - E\ (C_{60}) - E\ (Cd) \qquad\qquad (2)$$

where E (C_{60}) is the total energy for the isolated C_{60} molecule, E $(Cd\text{-}C_{60})$ is the total energy of the Cd atom occupying the centre of the C_{60} cage or interacting on the surface of C_{60} and E (Cd) is the total energy of cadmium atom (the reference state).

In order to calculate the encapsulation or association energy accurately, dispersion has been included by using the pair-wise force field as implemented by Grimme *et al.*[33] in the VASP package.

All the calculations have been performed at isobaric conditions (P=constant), thus no further thermodynamical corrections are necessary[34]. For example, the association energy depends on pressure and this has been well discussed by Varotsos [34a].

3. Results and discussion

3.1. Structure and electronic properties of C_{60}.

The starting point of the present study was to reproduce the experimental structure of C_{60} and compare its electronic structure with other theoretical studies to assess the quality of the pseudopotentials and basis sets used. Figure 1 represents the relaxed structure of C_{60}. In C_{60}, there are two different C-C bonds (C-C and C=C) present. The calculated bond lengths of C-C and C=C are 1.45 Å and 1.40 Å respectively in excellent agreement with corresponding experimental values of 1.43 Å and 1.39 Å[35]. The density of states (DOS)

(refer to Figure 1 b) calculated for C_{60} predicts that the energy gap between the highest occupied molecular orbital (HOMO) (see Figure 1 c) and the lowest unoccupied molecular orbital (LUMO) (see Figure 1 d) is 1.55 eV, in good agreement with the value of 1.64 eV calculated by Goclon *et al.*[36].

3.2. Formation of Cd interacting with C_{60}

First we consider the stability of Cd atom occupying inside the C_{60} cage. In the relaxed configuration, the position of the Cd atom remains very close to the centre of the cage. The encapsulation energy of Cd was calculated with and without dispersion and the corresponding encapsulation energy values are −0.18 eV and 0.55 eV respectively showing the necessity of including dispersion. Thus, in the following sections we only report the values calculated using dispersion. The encapsulation of Cd is exothermic with non-covalent nature. This is further supported by a small amount of charge transfer (0.10 |e|) from Cd to C_{60} according to the Bader charge analysis[37].

Next, we considered outer surface of the C_{60} for the interaction of Cd. Five different initial configurations (refer to Figure 2) were considered as shown in Figure 2. Table 1 reports the final configuration together with relative association energies and the Bader charge on Cd atom in the relaxed. The most stable site for the exohedral adsorption of Cd is 66. The association energy calculated for this site is −0.15 eV again showing the weak adsorption. The Bader charge analysis shows that the electronic configuration of Cd is unaltered. Recently, Sankar De *et al.*[19] have studied the adsorption of different element in the periodic table and reported the most stable sites for trapping. The lowest energy configuration found for Cd in their study is "bridge site" and they define this site as an atom on the C–C bond. Importantly, there are two possible C–C bonds [66 and 65] present in the C_{60}. Nevertheless, the difference in the energy between 66 and 65 is only 0.04 eV. Furthermore, they did not consider the dispersion correction and further, reports only the relative energies. Therefore, we are unable to compare the association energy of Cd with their value.

3.3. Structure and electronic properties of B, Si and N doped C_{60}

In order to improve the trapping of Cd at both inner and outer surfaces of the C_{60}, B, Si and N were substitutionally doped. The optimised structures of doped C_{60} are shown in Figure 3a. As discussed earlier, there are two types of C-C bonds, the C-C and the C=C present in undoped C_{60} with the bond distances of 1.45 Å and 1.40 Å respectively.

In the relaxed structure of C_{60} doped with B, B–C bond lengths (see Figure 3 b) are ~0.1 Å longer than the C–C bond lengths in the pristine C_{60} and are in good agreement with the

values calculated by Bai *et al.*[38] Also, there is a slight change in the C–C bond distances closer to the B. The Bader charge analysis shows that the boron donates its three outer electrons ($2s^2 2p^1$) to the nearest neighbour carbon atoms (see Figure 3 c) and becomes 3+ charge. The total DOS (see Figure 4 a) shows that doping with B introduces additional bands just above the HOMO of C_{60} and the band gap is reduced by 0.55 eV. The HOMO is mainly dominated by p-orbials of B as shown in Figure 4 b and Figure 5 a.

Silicon forms an outward relaxation with Si-C bond lengths between 1.79–1.84 Å, similar values obtained for Si substitutional doping in nanotubes[39] and fullerenes[38]. Silicon donates ~3.50 electron to the nearest neighbour carbon atoms as shown in Figure 3 c. The total DOS (see Figure 4 a) shows that the HOMO is dominated by valence p orbitals of C and Si as evidenced by DOS plotted for p states of Si. The longer Si–C distances shows that Si forms a single covalent bond with C and there is a vacant orbital available on Si for further bonding. This is reflected in the LUMO shown in Figure 5 b. Doping with Si reduces the HOMO-LUMO gap by 0.45 eV.

The opposite effect is observed for nitrogen. As nitrogen is more electro negative than carbon, N gains ~2.60 electron from its nearest neighbour Ca toms (see Barder charge approximation in Figure 3 c). There is a slight reduction in the bond distances (~0.03 Å). The Fermi energy is shifted to the higher values.

Next we calculated the substitutional doping energy by the following reaction;

$$E(C_{60}) \quad + \quad E(X) \quad \rightarrow \quad E(XC_{59}) \quad + \quad E(C) \qquad \qquad (1)$$
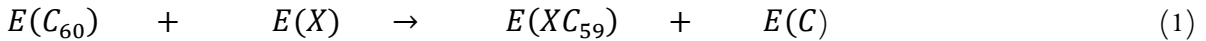
Where $E(C_{60})$ is the total energy of C_{60}, $E(X)$ is the energy of isolated dopant atom, $E(XC_{59})$ is the total energy of doped C_{60} and $E(C)$ is the energy of isolated C atom. Calculated substitutional doping energies for B, Si and N are 0.37 eV, 1.18 eV and 3.09 eV respectively. This indicates that B- doping is the lowest energy doping strategy.

3.4. Encapsulation of Cd within B,Si and N doped C_{60}

Thereafter, we calculated the encapsulation energy of Cd in the doped C_{60}. The encapsulation energies and the Bader charge on Cd are reported in Table 2. In all three relaxed structures Cd occupied closer to the centre of the cage. There is a slight enhancement in the encapsulation in B and Si doped C_{60} as evidenced by the Bader charge. This is due to the structural change in the cage by doping. Nitrogen shows almost encapsulation energy calculated with pristine C_{60}.

3.5. Trapping of Cd on the surface of doped C_{60}

Finally, we have considered the interaction of Cd on the surface of doped C_{60}. Different initial configurations were considered placing Cd at different positions above the dopant. However, all configurations prefered only one stable structure in each case and the final configurations are shown in Figure 6.

Both B and Si exhibit stronger attraction between with Cd. The associations energies (see Table 3) indicate that trapping capability of C_{60} doped with B or Si is approximately three times stronger than the pristine C_{60}. This is due to the polarisation of positively charged B or Si with closed shell $d^{10}s^2$ configuration of Cd. This is further evidenced by the Bader charges on Cd and dopants. In the case of N, there is a repulsion between electrons localised on N and closed shell configuration of Cd. This is further evidenced by the longer N-Cd bond length.

Total DOS's and atomic dos's for dopants and Cd are given in Figure 7. Top of the valence band calculated for Cd interacting B doped C_{60} is a mixture of p-states of B and s states of Cd. This is further supported by HOMO (refer to Figure 8 a). This is also the case for Cd interacting with Si doped C_{60} as evidenced by its DOS and HOMO. In the case of Cd interacting N doped C_{60}, s states of Cd is not contributed to HOMO (refer to Figure 8 and DOS in figure 7).

4. Conclusions

Using density functional theory together with a dispersion correction and vdW forces, we have investigated the capacity of C_{60} and B-, Si- and N- doped C_{60} to trap cadmium. The present calculations show that Cd is weakly trapped via van der Waals forces by C_{60} both endohedrally and exohedrally. Both B and Si doped C_{60} enhance the Cd encapsulation (trapping inside) slightly. However, significant enhancement in Cd trapping was observed on the outer surface of B and Si doped due to the attractive interaction with positively charged dopants and Cd. As the lowest substitutional energy is calculated for B, we conclude that B-doped C_{60} is the candidate material for the removal of Cd and experimental investigations should further confirm this.

Conflicts of interest

The authors declare that there is no competing financial interest.

References

1   M. Jaishankar, T. Tseten, N. Anbalagan, B. B. Mathew and K. N. Beeregowda, Interdisciplinary Toxicology, 2014, 7, 60-72.

2   L. Järup, British Medical Bulletin, 2003, 68, 167-182.

3   E. K. Leffel, C. Wolf, A. Poklis and K. L. White, Toxicology, 2003, 188, 233-250.

4   S. Guan, T. Palermo and J. Meliker, International Journal of Hygiene and Environmental Health, 2015, 218, 147-152.

5   N. Johri, G. Jacquillet and R. Unwin, BioMetals, 2010, 23, 783-792.

6   M. Tellez-Plaza, M. R. Jones, A. Dominguez-Lucas, E. Guallar and A. Navas-Acien, Current atherosclerosis reports, 2013, 15, 356.

7   W. Wang and V. Fthenakis, Journal of Hazardous Materials, 2005, 125, 80-88.

8   M. K. Jha, V. Kumar, J. Jeong and J.-c. Lee, Hydrometallurgy, 2012, 111-112, 1-9.

9   J. Nakajima, M. Fujinami and K. Oguma, Analytical Sciences, 2004, 20, 1733-1736.

10   P. Abiman, G. G. Wildgoose, A. Crossley and R. G. Compton, Electroanalysis, 2009, 21, 897-903.

11   M. A. Barakat, Arabian Journal of Chemistry, 2011, 4, 361-377.

12   M. Karnib, A. Kabbani, H. Holail and Z. Olama, Energy Procedia, 2014, 50, 113-120.

13   X. Wang, R. Qu, J. Liu, Z. Wei, L. Wang, S. Yang, Q. Huang and Z. Wang, Environmental Pollution, 2016, 208, 732-738.

14   M. R. Panuccio, A. Sorgonà, M. Rizzo and G. Cacco, Journal of Environmental Management, 2009, 90, 364-374.

15   J.-S. Chang, R. Law and C.-C. Chang, Water Research, 1997, 31, 1651-1658.

16   H. Dai, Accounts of Chemical Research, 2002, 35, 1035-1044.

17   Y. Wang, D. Tománek and R. S. Ruoff, Chemical Physics Letters, 1993, 208, 79-85.

18   N. Kuganathan, A. K. Arya, M. J. D. Rushton and R. W. Grimes, Carbon, 2018, 132, 477-485.

19   D. Sankar De, J. A. Flores-Livas, S. Saha, L. Genovese and S. Goedecker, Carbon, 2018, 129, 847-853.

20   E. Brocławik and A. Eilmes, Journal of Chemical Physics, 1998, 108, 3498-3503.

21   K. Kikuchi, K. Kobayashi, K. Sueki, S. Suzuki, H. Nakahara, Y. Achiba, K. Tomura and M. Katada, Journal of the American Chemical Society, 1994, 116, 9775-9776.

22   S. K. Saha, D. P. Chowdhury, S. K. Das and R. Guin, Nuclear Instruments and Methods in Physics Research Section B: Beam Interactions with Materials and Atoms, 2006, 243, 277-281.

23   A. K. Srivastava, S. K. Pandey and N. Misra, Materials Chemistry and Physics, 2016, 177, 437-441.

24   J. Lu, Y. Zhou, X. Zhang and X. Zhao, Molecular Physics, 2001, 99, 1199-1202.

25   S. C. Cho, T. Kaneko, H. Ishida and R. Hatakeyama, Journal of Applied Physics, 2015, 117, 123301.

26   H. Minezaki, K. Oshima, T. Uchida, T. Mizuki, R. Racz, M. Muramatsu, T. Asaji, A. Kitagawa, Y. Kato, S. Biri and Y. Yoshida, Nuclear Instruments and Methods in Physics Research Section B: Beam Interactions with Materials and Atoms, 2013, 310, 18-22.

27   N. Kuganathan, J. C. Green and H.-J. Himmel, New Journal of Chemistry, 2006, 30, 1253-1262.

28   J. R. Heath, S. C. O'Brien, Q. Zhang, Y. Liu, R. F. Curl, F. K. Tittel and R. E. Smalley, Journal of the American Chemical Society, 1985, 107, 7779-7780.

29   G. Kresse and J. Furthmüller, Physical Review B, 1996, 54, 11169-11186.

30   G. Kresse and D. Joubert, Physical Review B, 1999, 59, 1758-1775.

31   J. P. Perdew, K. Burke and M. Ernzerhof, Physical Review Letters, 1996, 77, 3865-3868.

32   W. H. Press, S. A. Teukolsky, W. T. Vetterling & B. P. Flannery, *Numerical recipes in C (2nd ed.): the art of scientific computing.* (Cambridge University Press, 1992).

33   S. Grimme, J. Antony, S. Ehrlich and H. Krieg, The Journal of Chemical Physics, 2010, 132, 154104.

34   (a) P. Varotsos, J. Appl. Phys. 101 (2007) 123503, (b) A. Chroneos and R.V. Vovk, Solid State Ionics 274 (2015) 1-3 and (c) A. Chroneos, Appl. Phys. Rev. 3 (2016) 041304.

35   J. M. Hawkins, Accounts of Chemical Research, 1992, 25, 150-156.

36   J. Goclon, K. Winkler and J. T. Margraf, RSC Advances, 2017, 7, 2202-2210.

37   G. Henkelman, A. Arnaldsson and H. Jónsson, Computational Materials Science, 2006, 36, 354-360.

38   H. Bai, W. Ji, X. Liu, L. Wang, N. Yuan and Y. Ji, Journal of Chemistry, 2013, 2013, 9.

39   R. J. Baierle, S. B. Fagan, R. Mota, A. J. R. da Silva and A. Fazzio, Physical Review B, 2001, 64, 085413.

Table 1. Initial and final configurations (refer to Figure 2 for definitions) of Cd absorbed on C_{60} exohedrally and Bader charge on Cd atoms. The most stable configuration is highlighted in bold.

Initial Configuration	Final configuration and relative association energy (eV)	Bader charge on Cd (|e|)
H	H, +0.02	+0.02
P	P, +0.04	+0.03
66	**66, +0.00**	+0.02
65	65, +0.04	+0.04
C	C, +0.05	+0.03

Table 2. Encapsulation energies of Cd incorporation inside the doped C_{60} and Bader charge on Cd

Doped C_{60}	Encapsulation energy (eV)	Bader charge on Cd ($|e|$)
B•C59	−0.23	+0.21
Si•C59	−0.25	+0.20
N•C59	−0.18	+0.21

Table 3. Association energies of Cd interacting outer surface of doped C_{60} and Bader charge on Cd and dopants.

Doped C_{60}	Association energy (eV)	Bader charge on Cd ($|e|$)	Bader charge on doptants ($|e|$)
B•C59	−0.51	+0.28	+3.00
Si•C59	−0.61	+0.20	+2.34
N•C59	−0.10	+0.02	−2.69
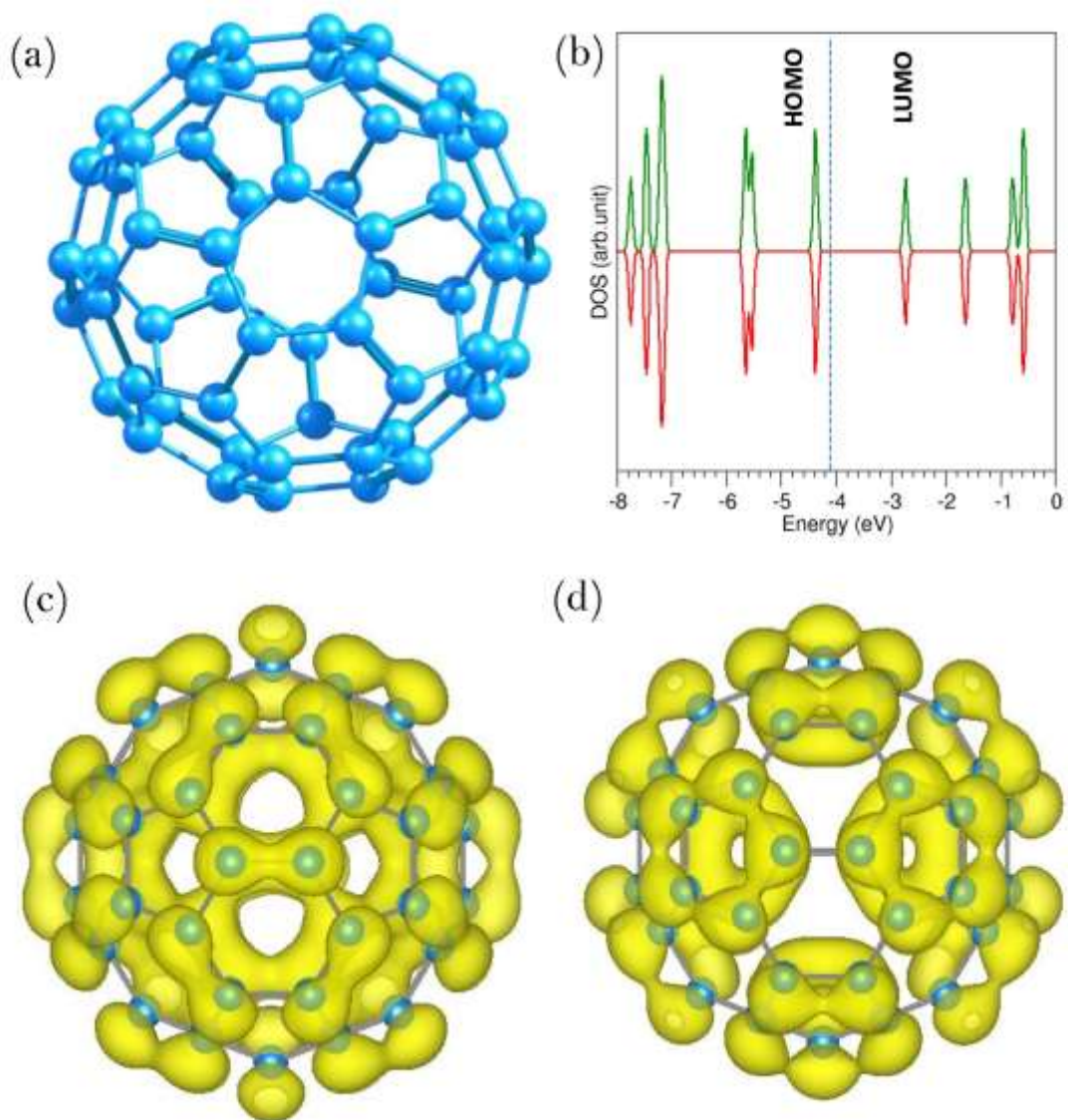
Figure 1. (a) Relaxed structure of C_{60} (b) total density of states of C_{60} and (c) and (d) charge density isosurfaces of HOMO and LUMO respectively. The vertical blue dotted line corresponds to the Fermi level.
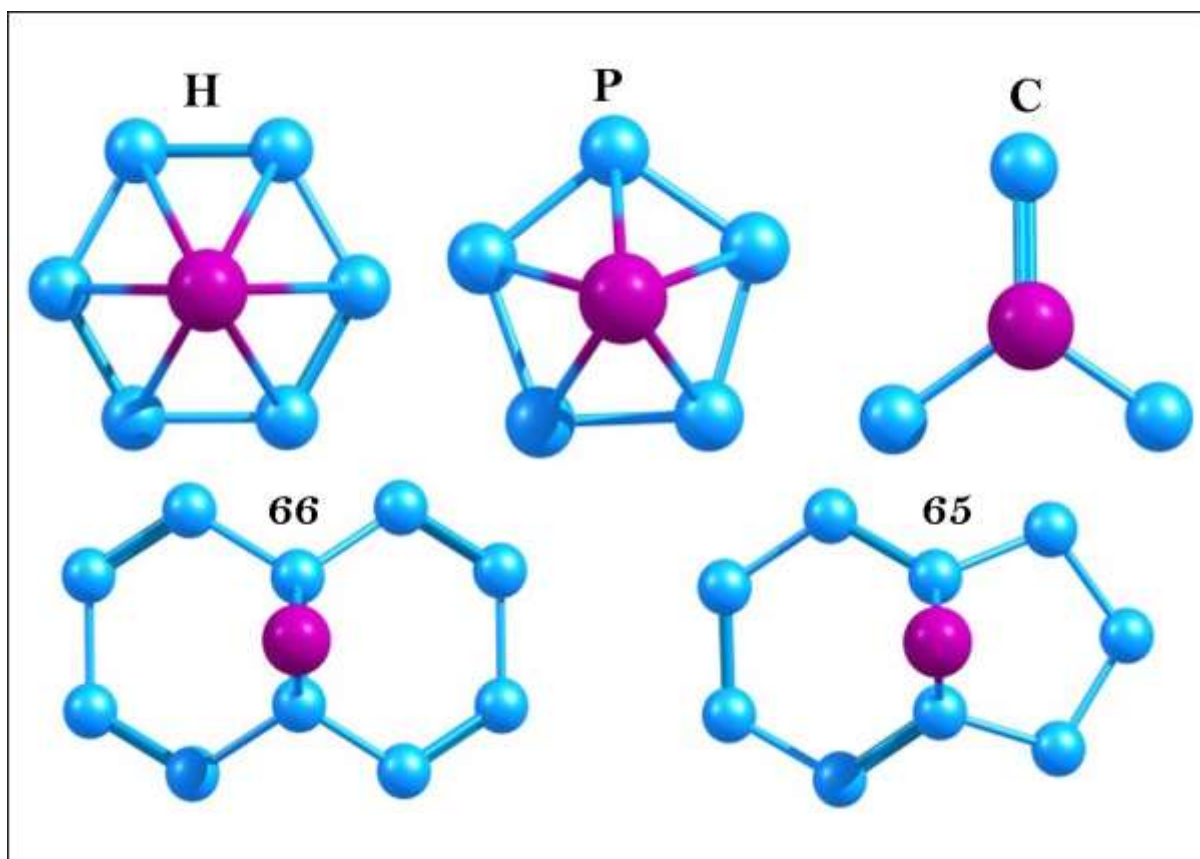
Figure 2. Initial configurations of Cd absorbed exohedrally.

13
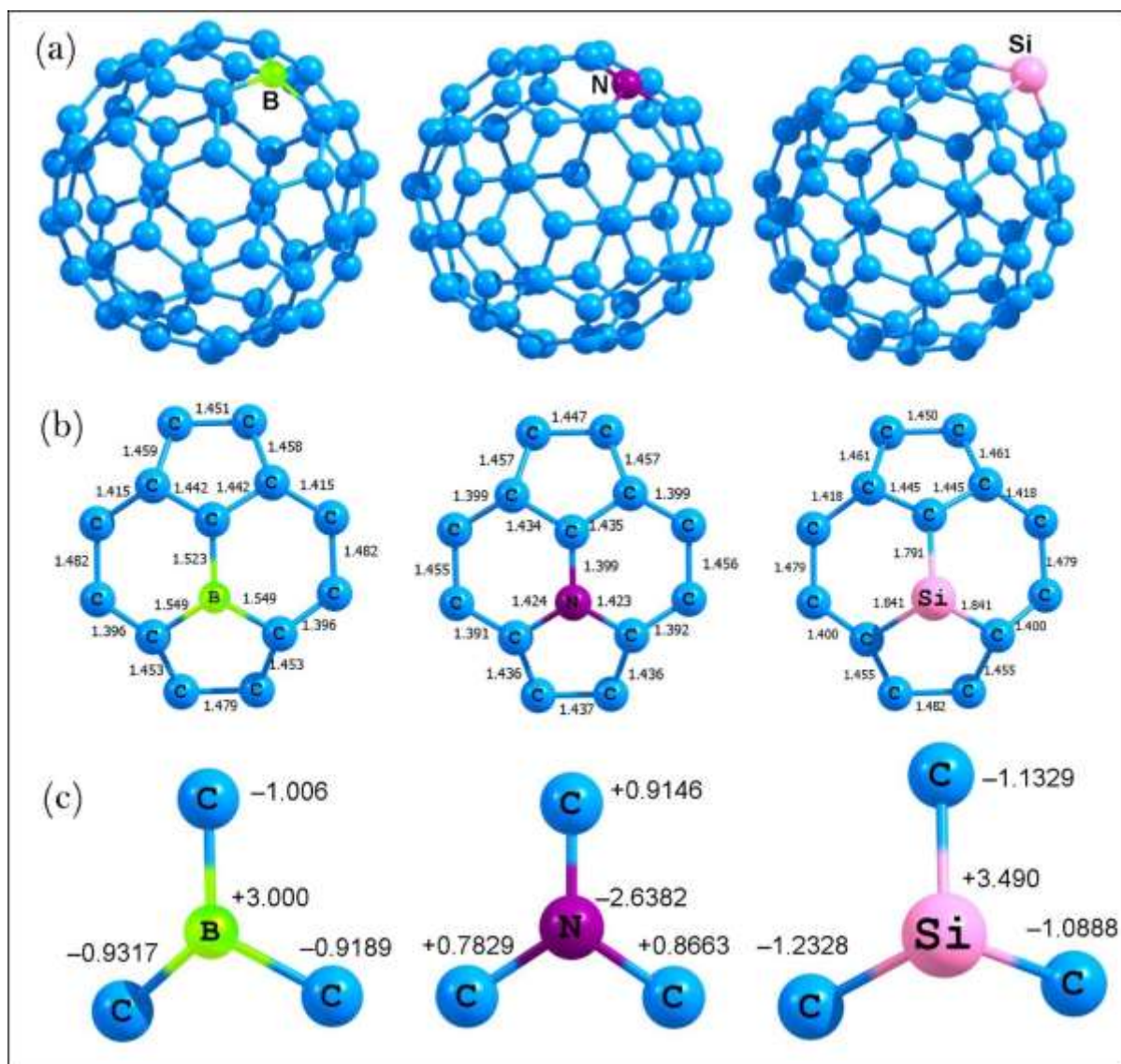
Figure 3 (a) Relaxed structures B, Si and N doped C_{60}, (b) bond distances closer to the dopants and (c) Bader charges on dopants and their nearest neighbour carbons.
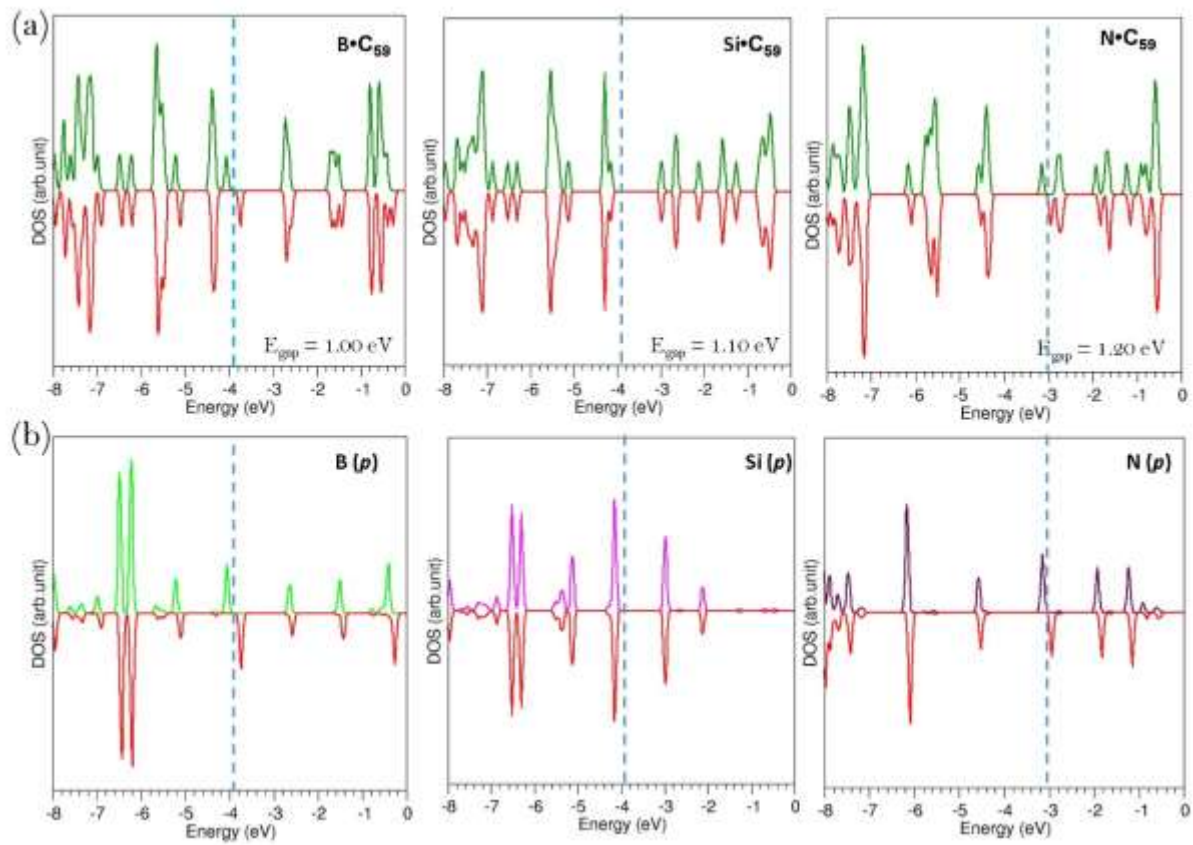
Figure 4. (a) Total densities of states of doped C_{60} and (b) p states of doped atoms. The vertical dotted lines correspond to the Fermi energy level.
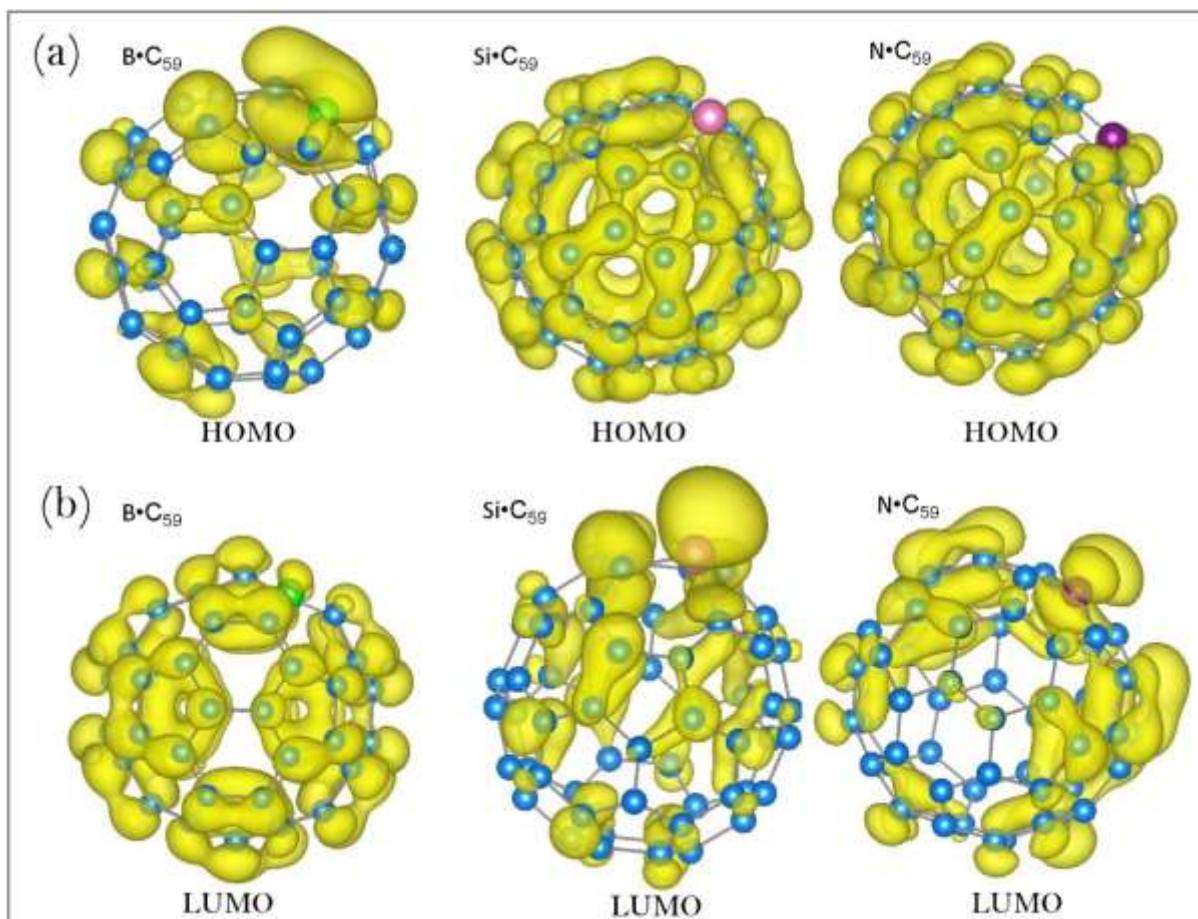
Figure 5. (a) HOMO and (b) LUMO iso-surface charge densities calculated for C_{60} doped with B, Si and N.
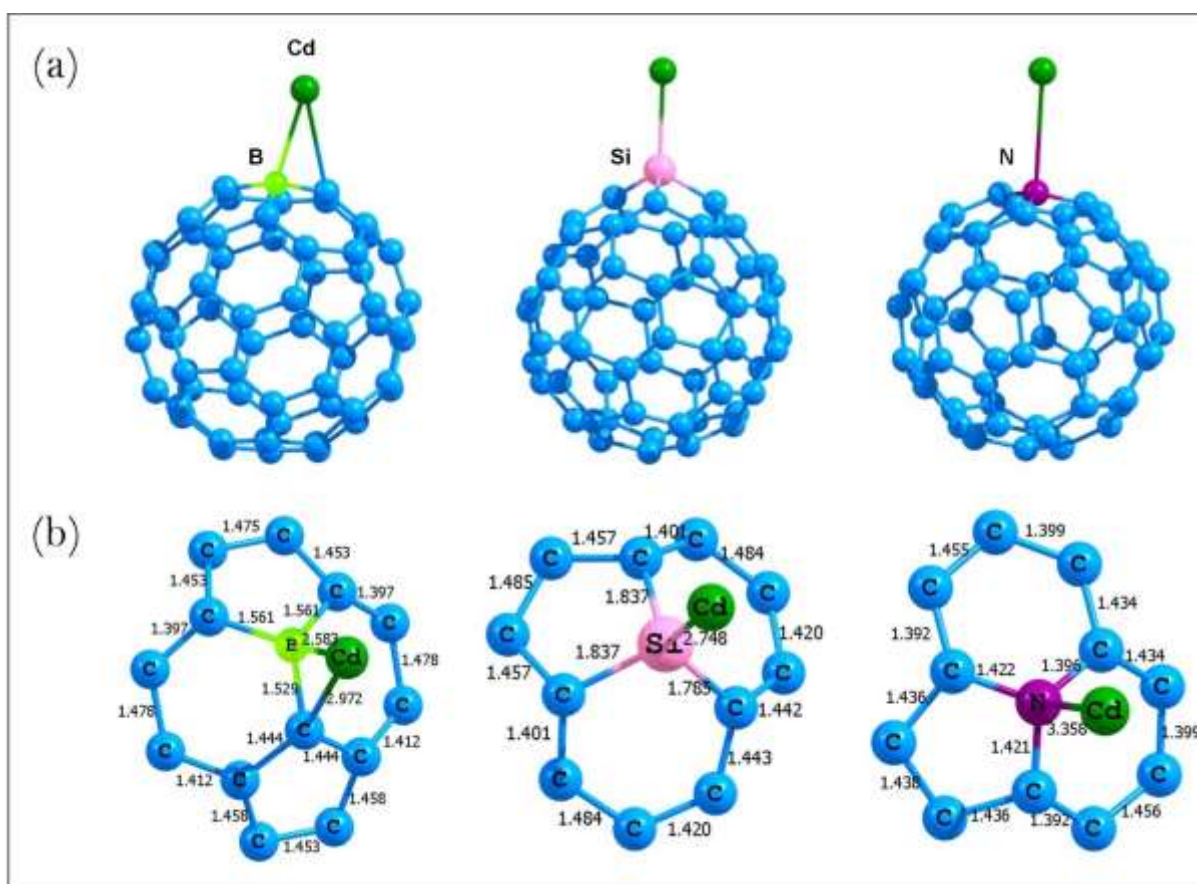
Figure 6 (a) Relaxed structures of Cd absorbed on doped C_{60} and (b) C–X and Cd–X (X= B, Si and N) distances
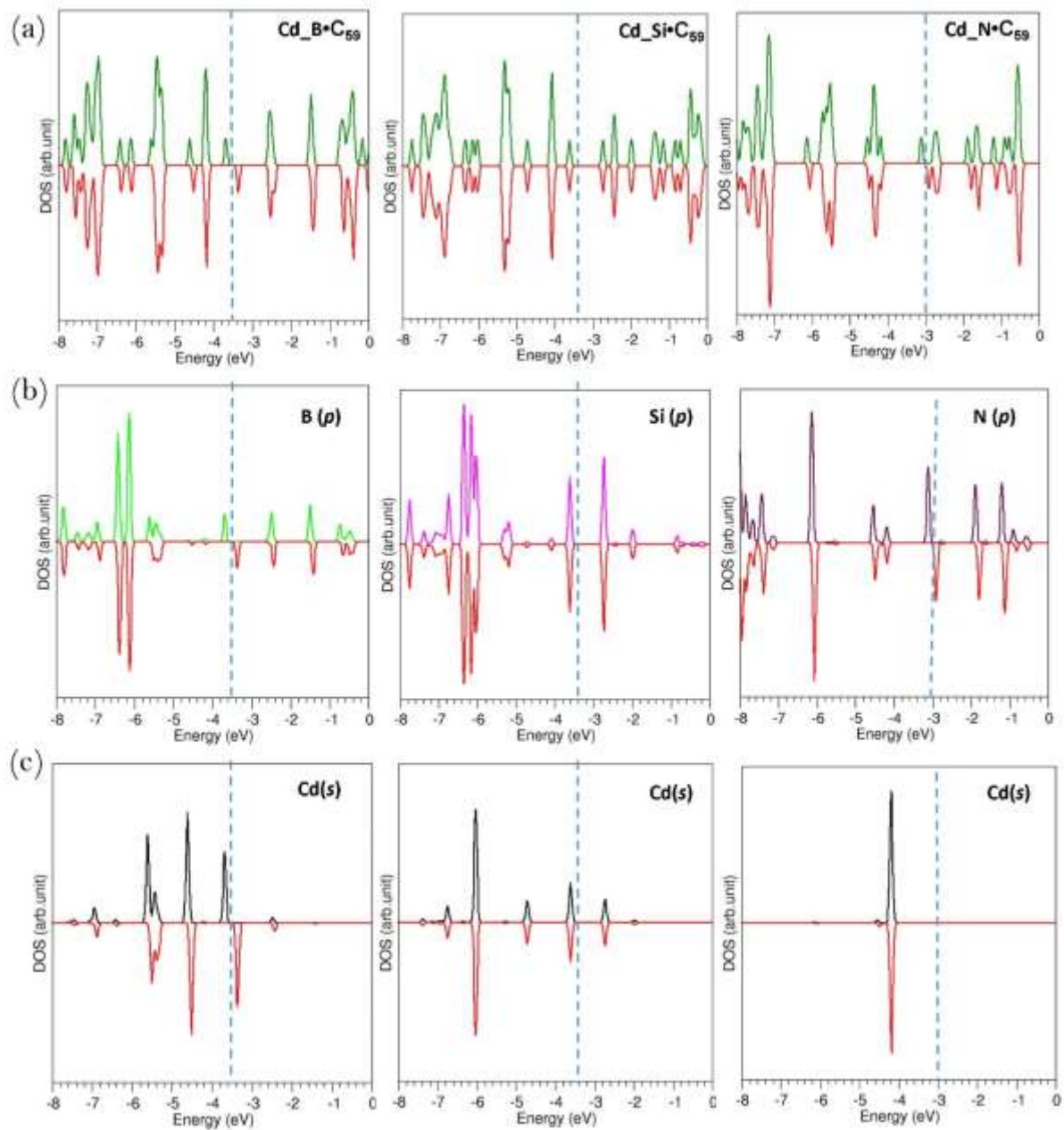
Figure 7. (a) Total densities of states of Cd interacting doped C_{60} and (b) p states of doped atoms and (c) s states of Cd. The vertical dotted lines correspond to the Fermi energy level.
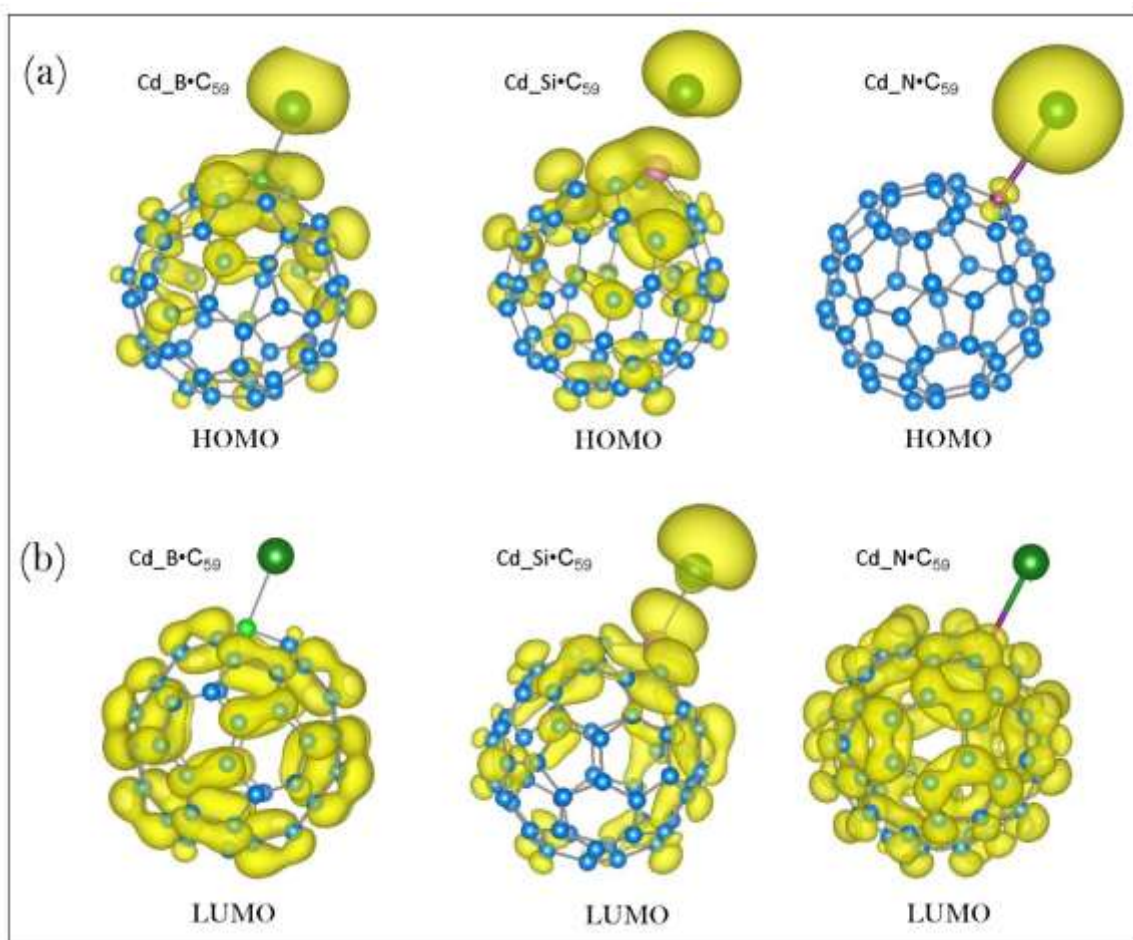
Figure 8. (a) HOMO and (b) LUMO iso-surface charge densities calculated for Cd interacting C_{60} doped with B, Si and N.